Tạp chí Khoa học và Công nghệ **52** (3) (2014) 357-372

SYNTHESIS AND COMPARATIVE PHOTOLUMINESCENCE OF CdZnSe / ZnS AND CdZnSe / ZnSeS ALLOY QUANTUM DOTS

Nguyen Hai Yen[1, *], Nguyen Ngoc Hai[1], Le Van Vu[2], Phan Tien Dung[1], Nguyễn Xuân Nghĩa[1], Laurent Coolen[3, 4], Pham Thu Nga[1]

[1]*Institute of Materials Science, Vietnam Academy of Science and Technology, 18 Hoang Quoc Viet Road, Cau Giay District, Hanoi, Vietnam*

[2]*Center for Materials Science, Faculty of Physics, Hanoi University of Natural Science - VNUH, 334 Nguyen Trai St., Thanh Xuan, Hanoi, Vietnam*

[3]*Sorbonne Universités, UPMC Univ Paris 06, UMR 7588, Institut de NanoSciences de Paris (INSP), F-75005, Paris, France*

[4]*CNRS, UMR 7588, Institut de NanoSciences de Paris (INSP), F-75005, Paris, France*

*Email: haiyen@ims.vast.ac.vn

Received: 27 November 2013; Accepted for publication: 19 March 2014

ABSTRACT

In order to search for new structures and compositions of quantum dots, suppress the blinking photoluminescence (random changes between high emission state (on) and low emission status (off) under continuous photo- excitation) and serve the application purposes in bio- medical and in optoelectronic devices , we have studied the fabrication of new alloy quantum dots (QDs). In this paper, we present new results on alloy core / shell quantum dots, with changed alloy shell composition, that was CdZnSe/$ZnSe_xS_{1-x}$ a ML with x (x = 0 , 0.2, 0.4, 0.5, 0.6, 0.8) and the shell thickness in monolayer (ML) (a = 2 , 4 , 6) . The emission spectra and the intensity change according to the composition of the alloy shell. The full width a half maximum (FWHM) of the emission spectra of quantum dots CdZnSe is 25.5 nm. Covered with a shell layer, the emission intensity of the CdZnSe core increases along with the shell thickness. For comparison purpose, two different shell materials have been used, which are ZnS and ZnSeS alloy. With the same shell thickness, the emission wavelengths and intensity of the QDs change when the shell's composition changes. The photoluminescence (PL) decay and the PL blinking of the alloy QDs was studied. It was shown that the alloy QDs spent by the nanocrystal in the ON state ranged typically between 20 and 40 %, and was dependent on the core composition. Detailed discussions on the experiment results are presented.

Keywords: alloy quantum dots, synthesis, nanocrystal, core/shell structure, photoluminescence, CdZnSe/ZnSeS.

1. INTRODUCTION

Colloidal semiconductor quantum dots (QDs) such as binary CdSe and CdTe, whose band gaps are continuously tuned by changing sizes, offer a new powerful tool for use in multicolor

bio-imaging, bio-sensing, light-emitting diodes, photovoltaic devices, lasers, and quantum computing devices [1 - 8]. In order to demonstrate short wavelength-emitting QDs, the QDs would have to be small enough to induce a strong quantum confinement effect. However, such small-size QDs are often highly unstable, inefficient, spectrally broad, and lacking in narrow-size distribution [9 - 12]. Instead of controlling the size of QDs, the formation of alloy (solid solution) QDs can be an alternative approach to tune their energy band gaps, typically using ternary or quaternary compositions such as $Zn_xCd_{1-x}Se$ [9 - 15], $Zn_xCd_{1-x}S$ [16 - 18], $CdSe_{1-x}Te_x$ [19] and $Zn_xCd_{1-x}Se_yS_{1-y}$ [20]. In these multi-compositional QDs, the band gap energy of the QDs is determined by the combination of their chemical stoichiometry and particle size. Alloy QDs have been achieved by (i) heating core/shell-structure QDs to an appropriate temperature, thus replacing the cation of pre-prepared binary QDs [9 - 11] or changing the constituent cation/anion precursor amounts of the QDs [12, 17, 18]. Recently, several groups have demonstrated that alloy QDs have many advantages over binary QDs. For example, Bawendi and co-workers [21] fabricated LEDs using ZnCdSe ternary-alloyed QDs, which enabled easier charge injection than in CdSe/ZnS QDs. Krauss et al.[22] described "non-blinking" CdZnSe/ZnSe QDs that have an alloy composition. Furthermore, the nature of the blinking phenomenon was discussed in refs. [23, 24]. These findings indicate that alloy QDs may represent a new route to achieve the next generation of QDs [2, 25]. The widely tunable emissions of $Zn_xCd_{1-x}Se$ alloy quantum dots (QDs), which emit green to red wavelengths from 534 to 620 nm, are reported [1]. The compositions of alloy QDs were estimated based on their sizes and band gap energy.

Among all the steps required to synthesize quantum dots, the generation of the outer inorganic layer is the most critical one for producing highly emissive materials. The best materials contain a "shell" of wide band gap material that wraps around the "core" quantum dot; among other functions, this layer ensures that the materials possess the exceedingly high and stable quantum yields which are pivotal for their many applications. The importance of shell layers was first identified by Hines *et al* in 1996 who demonstrated an improvement in the quantum yield and stability of CdSe nanocrystals after coating with ZnS [26, 27]. Thanks to that effort, virtually all types of quantum dots have been prepared with appropriate shells and core–shell systems, which are now the default structures for quantum dots. Shell thickness could be manipulated by changing the reaction temperature and time or through a more conventional strategy of multiple precursor injection.

For comparison purpose, in this work, two different shell materials have been used, which are ZnS and ZnSeS alloy. We have synthesized monodisperse ZnS and ZnSeS shells on CdZnSe alloy quantum dots at temperatures as 240 ^oC to form thicker shells, up to 6 monolayers (ML). II-VI ternary composition-alloy QDs with core/thick shell structure in which band gaps can be engineered over the entire visible spectrum have not been reported yet to date. Herein, we report on the synthesis of good quality ternary alloy $Cd_{0.4}Zn_{0.6}Se/ZnS$ aML and $Cd_{0.4}Zn_{0.6}Se/ZnSe_xS_{1-x}$. aML (with x = 0, 0.2, 0.4, 0.5, 0.6, 0.8 and a = 0, 2, 4, 6 ML) QDs by replacing the cation of pre-prepared binary QDs, and on the structural characterization and photoluminescence of these ternary alloy quantum dots. When covered with one shell layer, the emission intensity of the CdZnSe core increases along with the shell thickness. For alloy shell like $ZnSe_xS_{1-x,}$ with the same shell thickness, the intensity and emission wavelength of the QDs change when the shell's compositions change, the emission peak is shifted to red. By PL microscopy, the PL blinking of the obtained alloy QDs was studied. Discussions on the experiment results are also presented.

2. EXPERIMENTAL

2.1. Chemicals

The following reagents were used: cadmium acetate ($Cd(AC)_2$, 99.9 %), zinc acetate ($Zn(Ac)_2$, 99.9 %), selenium powder (Se, 99.99 %), hexamethyl disilthiane $(TMS)_2S$, trioctylphosphine oxide (TOPO, 99 %), trioctylphosphine (TOP, 90 %) and hexadecylamine (HDA, 99 %) were purchased from Aldrich. For the purification step: methanol, toluene, chloroform and hexane were purchased from Merck. All chemicals were used without further purification.

2.2. Synthesis of $Cd_{0.4}Zn_{0.6}Se/ZnS$ and $Cd_{0.4}Zn_{0.6}Se/ZnSe_xS_{1-x}$ alloy nanocrystal core/shell quantum dots

In this report, we will present the QDs that were synthesized with a constant precursor ratio of 0.2 Cd/0.8Zn and we obtained the $Cd_{0.39}Zn_{0.61}Se$ alloy nanocrystal QDs (or $Cd_{0.38}Zn_{0.62}Se$) as it would be accurately determined with the EDS element analytical method that we will present in the next part. The first thing is the need to synthesis the alloy cores. The method for CdZnSe quantum dots synthesis is slightly adapted from existing work for CdSe QDs [28]. All synthetic routes are carried out using standard airless procedures. The reaction was run under ultra-pure nitrogen flow.

For a typical synthesis of 0.5 mM $Cd_{0.4}Zn_{0.6}Se$ alloy nanocrystal QDs, we use the molar ratio of the used precursors in the reaction is: Cd / Zn / Se = 0.2 / 0.8 / 3.33; TOPO / HDA = 55/45. Alloy core fabrication process is performed through two steps:

Step 1: Preparation of precursor solutions

Dissolve 0.025 g of cadmium acetate in 0.54 mL TOP at the temperature of 80 ^oC in nitrogen gas. When the $Cd(Ac)_2$ salt is completely dissolved in the TOP, we obtain a transparent solution, which is the TOP-Cd precursor solution that would be used for the reaction. After that, dissolve 0.0875 g of $Zn(Ac)_2$ in 1 ml TOP at the temperature of 140 ^oC, in nitrogen atmosphere. When $Zn(Ac)_2$ is dissolved in the TOP, we obtain a transparent solution, which is the TOP-Zn precursor solution that would be used for the reaction. For Se precursor, dissolve 0.135 g Se in 1.665 ml of TOP at 120 ^oC in nitrogen gas to remove all air and oxygen. When Se powder is completely dissolved in TOP, we obtain a colorless transparent liquid which is the TOP-Se precursor.

Step 2: Synthesic of CdZnSe alloy QDs samples

Pour 3.325 g TOPO and 1.6625 g of HDA into the three-neck reaction flask. Use nitrogen gas to remove water vapor and oxygen out of the reaction flask at room temperature for 30 min, then at 120 ^{o} C for one hour. Inject TOP-Se precursor into the flask under vigorous stirring and heating at temperatures up to 100 ^oC in N_2 atmosphere. Continue to stir and heat the reactor up to 190 ^oC, at this moment, inject TOP-Zn precursor solution into the reaction flask. Then increase the temperature of the flask up to 270 ^oC, at which inject TOP-Cd precursor into the reactor. As the temperature of the liquid in the reaction flask drops to ~ 260 ^oC, the nucleation of CdZnSe alloy quantum dot nanocrystals starts shaping quickly. Grow CdZnSe alloy quantum dots for 20 minutes or 28 min at a temperature of 280 ^oC – 290 ^oC, we obtain CdZnSe alloy QDs core.

2.2.1. Synthesis of a ZnSeS shell on the $Cd_{0.4}Zn_{0.6}Se$ core quantum dots

The final step in the process was shelling of the CdZnSe ternary cores. The molar ratio of the used precursors for growing the shell is: Zn / Se / S = 1.37 / 0.6 / 0.4. The shells are grown following a modified version of the successive ion layer adsorption and reaction (SILAR) procedure from [28 - 30], originally described by Peng and colleagues [31].

Use 0.25 mM (corresponding to 4 ml) of as-prepared crude CdZnSe alloy quantum dots put into three-neck flask, then fill the flask with nitrogen gas. The crude liquid has the substances such as TOPO and HDA in it. Then the mixture is evacuated for one hour at 50 °C. After evacuation, raise the temperature to 240 °C and the shell growth is processed under nitrogen flow. Several 10-minute delays between injection steps are necessary to produce multi-shell QDs. A little amount of the sample is extracted after the growth of each shell for optical measurements. The amount of precursors to be injected and expected shell thickness are calculated as reported in [28, 30]. Carry out the creation process of the ZnSeS alloy shell on CdZnSe QDs at a temperature of 240 ^oC as following:

Preparation of precursor solutions for shell growth: zinc acetate, TOP-Se and hexamethyl disilthiane $(TMS)_2S$ are used as zinc, selenium and sulfur source for ZnSeS (or ZnS) shell growth on CdZnSe plain cores in this study. A TOP-Zn stock solution is prepared by mixing 0.165 g of $Zn(Ac)_2$ and 1.88 ml of TOP, then heated to ~ 140 ^oC in N_2 atmosphere until a clear solution is formed. The concentration of the mixture liquid is 0.4 M. For TOP-Se, dissolve 0.026 g Se in 0.33 ml TOP, at a temperature of ~ 120 ^oC in N_2 gas atmosphere. It is important that the solution should stay clear after it is cooled to room temperature. For ZnSeS shell growth, TOP-Se is mixed with $(TMS)_2S$ (Se/S molar ratio = x/1-x; x= 0.2, 0.4, 0.5, 0.6 and 0.8).

Mix TOP-Se with 0.046 ml $(TMS)_2S$. Inject TOP-Zn precursor drop-by-drop very slowly (at a rate 1 to 2 drops/ second), under vigorous stirring of the liquid, then add the mixture of $(TMS)_2S$ and TOP-Se to the alloy QD core solution. After the end of each turn of TOP-Zn precursors and (TOP-Se & S^{2-}) mixture's injection, keep the reaction temperature at 240 ^oC and stir strongly in N_2 atmosphere for 15 minutes so that ions can have enough time to stick to the outer layer of the alloy quantum dots CdZnSe shell, thus forming single-layers and giving best reaction productivity. The time for alloy $ZnSe_xS_{1-x}$ shell growth is 15 minute. At the end of this step we obtain the CdZnSe/ZnSeS quantum dots and the expected shell thickness is 4 ML. In this experiment, the amount of chemicals for the shell calculated for the estimated cores size is about 7 nm. After the core/shell alloy quantum dots reach the desired emission wavelength, the heater is removed and the reaction mixture is cooled down to stop the reaction. When the temperature of the reaction mixture cools to below 70 ^oC, the alloy nanocrystals are dispersed in organic solvent (such as chloroform and toluene etc.).

2.2.2. Method of covering CdZnSe alloy quantum dots with ZnS shell

Similar to the method of covering alloy core with ZnSeS shell, but the temperature to grow the ZnS shell is 220 ^oC (lower than ZnSeS alloy shell), the amount of S put into the reactor is 0.115 ml. The result is the obtain of CdZnSe/ ZnS quantum dots (the amount of Zn/S used has ratio of 1.37/1) and the expected shell thickness is 2, 4, 6 ML depending on the amount of Zn precursor and S solution added.

2.3. Characterization of CdZnSe/ZnSeS alloy nanocrystal quantum dots

All the QD samples are diluted with chloroform or toluene. A methanol is used to precipitate the nanocrystal quantum dots in toluene solution, which are isolated by centrifugation and decantation. The excessive ligands and reaction precursors are removed by extensive purification prior to transmission electron microscopy (TEM), powder x-ray diffraction (XRD) and energy dispersive x-ray spectroscopy (EDS) measurements. The elemental analysis is carried out using a scanning electron microscope (SEM) equipped with an energy dispersive x-ray spectroscopy which revealed the presence of Zn, Cd, S, and Se in the sample composition. TEM specimens are made by evaporating one drop of alloy QDs toluene solutions on carbon-coated copper grids. The TEM micrographs are taken by JEOL JEM 1010 transmission electron microscope operating at an accelerating voltage of 80 kV. The XRD patterns of the alloy QDs are recorded by a Siemens D5005 x-ray powder diffractometer. The samples are prepared by evaporating a highly concentrated solution of nanocrystals onto a Si wafer substrates. The photoluminescence (PL) spectra are taken by using a Microspec 2300i spectrophotometer (USA) This measuring system is equipped with a He-Cd laser, which emits two wavelengths at 442 nm and 325 nm and used as the optical excitation source. The PL measurements were performed also by photonic excitation at 380 nm, 400 nm or at 453 nm, which was obtained with a dye laser (Laser Photonics LN102, Coumarine 420) pumped by a pulsed nitrogen laser (Laser Photonics LN 1000, 0.15 mJ energy per pulse, pulse width 0.6 ns.

3. RESULTS AND DISCUSSION

In fabricating alloy quantum dots, it is crucial to use the method allowing the creation of quantum dots with real alloy compositions. Therefore, the method used to determine the crystalline phase and composition of elements is important. Based on the existing experience of preparing thick and ultra-thick shelled CdSe/ZnS quantum dots, we have used a method similar to that for producing the alloy quantum dot type $Cd_{0.4}Zn_{0.6}Se/ZnS$. aML (series N4, N6, N7 and N8) and $Cd_{0.4}Zn_{0.6}Se/ZnSe_{0.5}S_{0.5}$. aML (a = 0, 2, 4, 6 ML) (series N9) [28]. These two sample series have same alloy core composition, but over-coated with two different shell types, with the same corresponding coating thickness. In addition, we also fabricate the sample system $Cd_{0.4}Zn_{0.6}Se/ZnSe_xS_{1-x}$ 4ML (x = 0.2; 0.4; 0.5; 0.6 and 0.8) (series N12 and N13). The purpose of the study of this sample series is to compare the luminescent properties of alloy core QDs when coated with the same alloy shell thickness (4 ML), but changed alloy shell composition. With this sample series, we have observed the emission color and also observed that luminescence intensity varies with the change of shell composition. We will analyze the structural characteristics of the sample series in succession.

3.1. Structural characterization

Figure 1 shows the powder X-rays diffraction (XRD) patterns of $Cd_{0.4}Zn_{0.6}Se$ cores samples (curves: 1-3) and core/shell structure, the shell being ZnS with different thickness: $Cd_{0.4}Zn_{0.6}Se/ZnS$ aML (a = 2, 4, 6 ML) (curves: 4 - 6) together with the indexing of major peaks. Three curves 1, 2 and 3 corresponding to the $Cd_{0.4}Zn_{0.6}Se$ core QD samples, with crystalline growth time: for 28 minutes (curve 1) and 20 minutes (curve 2) at 280 ^oC. Curve 3 is the CdZnSe core sample prepared at lower temperature (240 ^oC) for 18 min. The XRD patterns of $Cd_{0.4}Zn_{0.6}Se$ nanocrystal cores exhibit the characteristic peaks of zinc-blend (zb) II–VI semiconductor compounds.The peak positions are in between the ones of the corresponding

peaks of bulk zb CdSe (JCPDS 19-0191 data) and ZnSe (JCPDS 37-1463). In these samples, the two components CdSe and ZnSe differ only in the cations. As the group II cations diffuse much easier than the group VI anions in II-VI semiconductors, the Cd^{2+} and Zn^{2+} can be intermixed to form an alloy. As the Zn^{2+} content increased, the diffraction peaks shifted toward the higher-angle side compared with the pattern of pure CdSe. This shift is consistent with the ionic radius of Cd^{2+} (0.97 Å) being larger than that of Zn^{2+} (0.74 Å). This also indicates that Zn^{2+} entered into the framework of CdSe and formed a solid solution. Broad XRD peaks are attributed to the absence of long-range order in the materials and imply a small particle size. For the case of overcoating with the ZnS shell, the diffraction peaks gradually shift toward larger angles (curves 4 - 6) and were characteristic peaks of zinc-blend ZnS (JCPDS 5-566).

From XRD patterns of core/shell samples, we can be seen that, when over-coated a ZnS shell with thickness of 2 ML, we observed the ZnS cubic crystalline phase for QD samples. For the thicker ZnS shell, the samples with ZnS 4ML and 6ML, we observe the ZnS cubic phase clearer (curves 4,5). So it can be concluded that, when CdZnSe quantum dots are coated by ZnS shell, 2 ML or more, up to 6 ML, we observed crystalline phase of the ZnS shell (curve 6).

The composition of the QD samples is measured by energy dispersive X-ray (EDS) (Figure 2). It has to be noted that prior to these experiments, very careful purification of the samples is necessary in order to remove any unreacted metal precursor. EDS analysis indicates that subsequent incorporation of zinc into the crystal lattice takes place after reaction times ($\geq$ 18 min) and formation of $Cd_{0.4}Zn_{0.6}Se$ alloy nanocrystals is observed. Finally, a comparison of the results of EDS analysis of a sample taken after 20 min reveals that the global composition remains stable within the experimental precision throughout the reaction to the homogeneous alloy. Elemental analysis of ensembles of QDs reveals the presence of Zn, Cd and Se for the ZnCdSe core (Fig. 2, in top) and the presence of the three elements Zn, Se, and S in all four samples for the core/shell samples (Fig. 2, in below). The small peaks at ~1.7 and 2.0 keV correspond to Si (substrate) and P (surface ligands), which respectively still exist in the QDs sample.

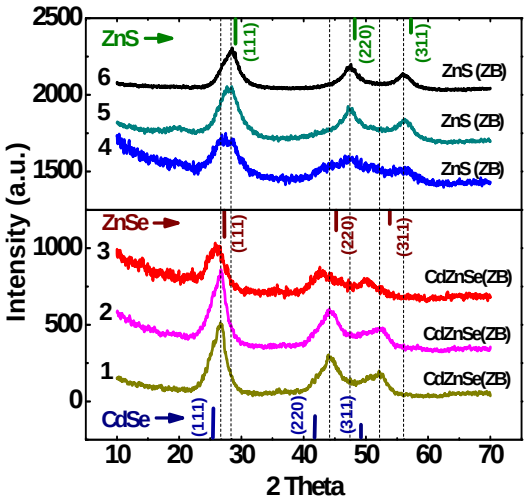

Figure 1. XRD patterns of the alloy nanocrystals QD samples on Si wafer substrates, with different shell thickness: from bottom to top: (1) $Cd_{0.4}Zn_{0.6}Se$ (reaction time-28 min), (2) $Cd_{0.4}Zn_{0.6}Se$ (reaction time-20 min), (3) CdZnSe (240 ^{o}C, 18 min), (4) $Cd_{0.4}$ $Zn_{0.6}Se$/ZnS 2ML, (5) $Cd_{0.4}$ $Zn_{0.6}Se$/ZnS 4ML,and (6) $Cd_{0.4}$ $Zn_{0.6}Se$/ZnS 6ML.

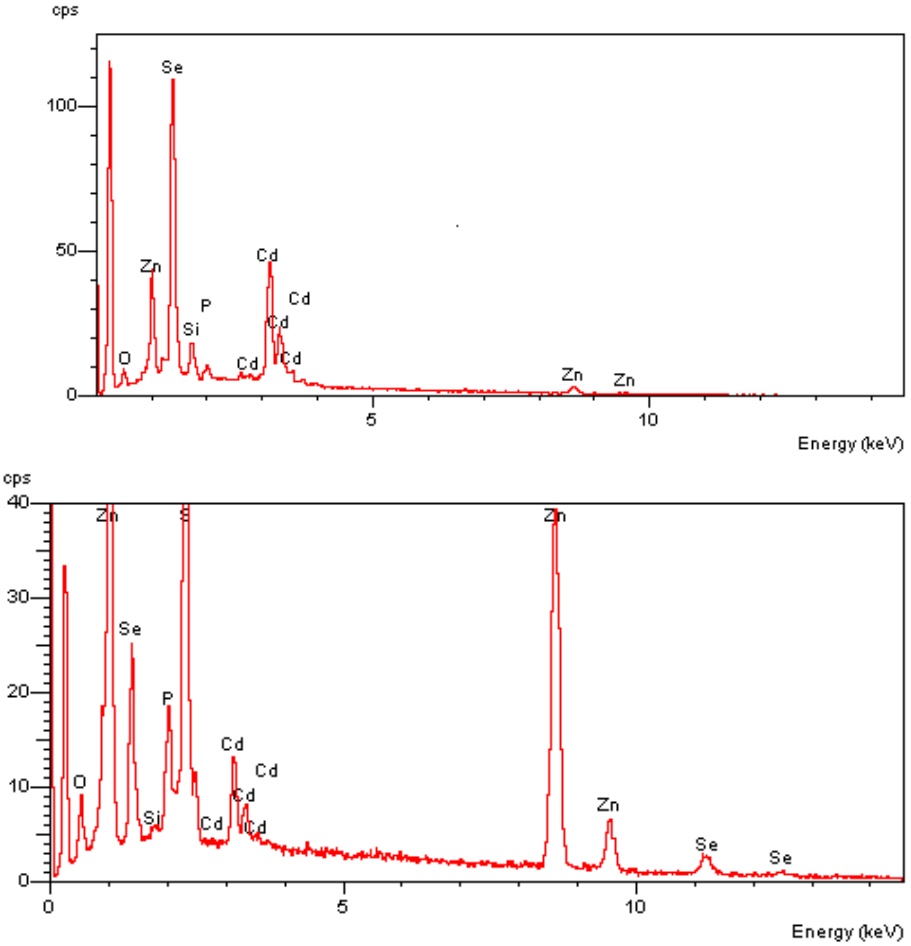

Figure 2. EDX spectra of $Cd_{0.4}Zn_{0.6}Se$ quantum dots (on top) and $Cd_{0.4}Zn_{0.6}Se/ZnS$ 4ML (below)

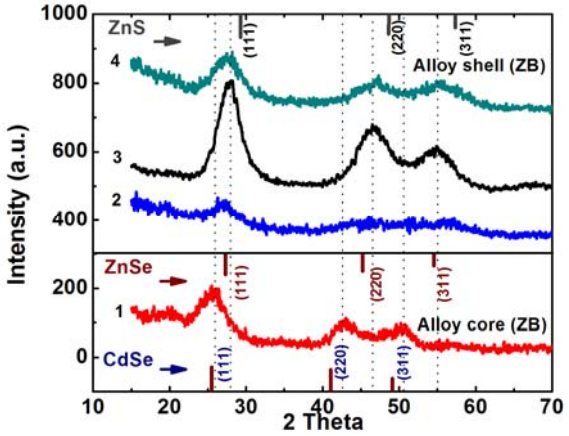

Figure 3 . XRD patterns of the alloy nanocrystals QD samples, with the same shell thickness: from bottom to top: (1) $Cd_{0.4}Zn_{0.6}Se$ core (2) $Cd_{0.4}Zn_{0.6}Se/ZnSe_{0.2}S_{0.8}$. 4ML (3) $Cd_{0.4}Zn_{0.6}Se/ZnSe_{0.5}S_{0.5}$. 4ML and (4) $Cd_{0.4}Zn_{0.6}Se/ZnSe_{0.6}S_{0.4}$.4ML.

We have carried out the analysis of important sample series whose results on crystalline

phase (with XRD patterns) had been analyzed and presented as above (Fig. 1), and will be presented in the following part (Fig. 3). The results on analyzing the elements in the samples, for example series N8 and N12 with the EDS method give the composition: the cores sample N8-0-12 have the composition $Cd_{0.39}Zn_{0.61}Se$ and the composition of cores sample N12-0-12 is $Cd_{0.38}Zn_{0.62}Se$.

Figure 3 is the XRD patterns of the samples series of alloy core/alloy shell structure, that was $Cd_{0.3}Zn_{0.6}Se/ZnSe_xS_{1-x}$. 4ML (x = 0.2, 0.5, 0.6). The shell thickness is 4 ML for all samples. The curves 1 is the XRD pattern of $Cd_{0.38}Zn_{0.62}Se$ alloy core sample, the diffraction peak positions are in between the ones of the corresponding peaks of bulk CdSe (JCPDS 19-0191 data) and ZnSe (JCPDS 37-1463 data). It seems they exhibit the characteristic peaks of zinc-blend closer with zb- CdSe. The curves 2-4 are XRD patterns of the core/alloy shell samples. The diffraction peaks shift toward the higher-angle side compared with the pattern of pure zb-ZnSe. Their position is between the ones of the corresponding peaks of bulk ZnSe (JCPDS 37-1463 data) and the characteristic peaks of zinc-blend ZnS (JCPDS 5-566). This confirms that the shell is alloy ZnSeS (curve 3 is the most obvious one).

TEM images of representative alloy QDs are shown in Figure 4 (a-b). The average sizes of alloy QDs core grown for 20 min are measured to be about 7 nm.

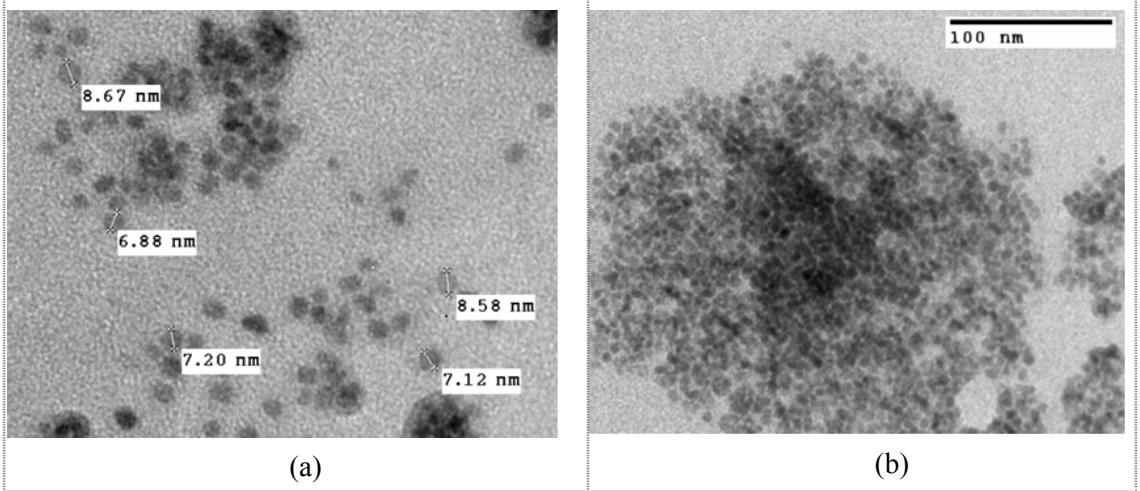

Figure 4. TEM images of the alloy QDs samples of $Cd_{0.4}Zn_{0.6}Se$ cores.

3.2. Photoluminescence measurement

3.2.1. Photoluminescence of $Cd_{0.39}$ $Zn_{0.61}Se/ZnS$. aML quantum dots

The PL spectra of $Cd_{0.39}Zn_{0.61}Se$ core, $Cd_{0.39}Zn_{0.61}Se/ZnS$ aML (a = 2, 4, 6 ML) is shown in Fig. 6. In general, the emission spectrum of the alloy QDs samples is a wide band. When a ZnS shell is coated on the core surface, the fluorescence intensity increased dramatically, and increases with the thickness of the applied layer, the peak position and spectrum width change not so much. They behave in the same manner, with a PL increase and redshift as the ZnS shell is grown. This indicates that the ZnS shell improves the properties by protecting the CdZnSe core from its environment. The emission spectra are however broader for these samples, which may indicate the presence of more inhomogeneities in these samples. Current work is under way in order to improve the synthesis of these materials. This is clearly observed even with the naked

eye, and through the quantitative measurement of photoluminescence spectra (Fig. 5). The emission peak is ~ 544 nm for the core sample to 549 nm for all samples QDs with the ZnS shell. Their emission intensity measured in the quantitative comparison form. The sample coated with ZnS shell as thick as the smaller concentrations than the original core samples. This allows us quantitative comparison of fluorescent intensity between the samples in the same series. The growth of the ZnS shell was accompanied by a significant increase in PL intensity (Fig. 5). This increase is observed by M. Protiere and P. Reiss [32]. Due to the lower lattice mismatch in the $Cd_{0.39}$ $Zn_{0.61}Se$/ZnS core/shell nanocrystals, the increase of PL intensity is still occur at much larger shell thicknesses up to 6 monolayers, as observed in the case of CdSe/ZnS thick shell QD [28]. For instance, as reported by Nie and colleagues, lattice strain can induce significant bandgap energy changes when a shell material is coherently grown on a small and compressible nanocrystalline core [33].

Let us now consider the decay of the $Cd_{0.39}Zn_{0.61}Se$ /ZnS.aML nanocrystals at room temperature (Fig. 6). The $Cd_{0.39}$ $Zn_{0.61}Se$ core shows a decay time of typically 20 ns with a small component of 150 ns. The core/shell samples show a decay time of typically 30 ns, with also a slower time constant of 150 ns. The increase of the decay time from 20 to 30 ns with addition of a ZnS shell may be attributed to a decrease of the non-radiative decay channels related to surface states.

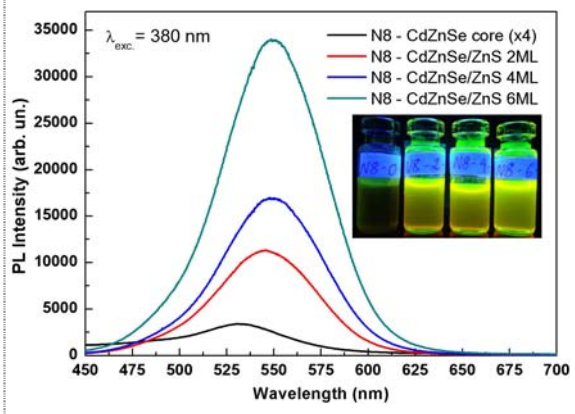

Figure 5. The PL spectra of $Cd_{0.39}Zn_{0.61}Se$ core, CdZnSe/ZnS aML (a = 2, 4, 6 ML) synthesized at 280°C (inset upper shows the normalized PL, inset below shows nanocrystals under UV light. From left to right: CdZnSe core, CdZnSe/ZnS 2ML, 4ML and 6ML).

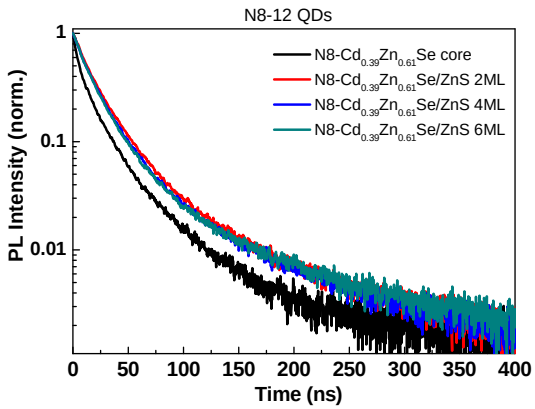

Figure 6. Time-resolved PL decay curves of $Cd_{0.39}Zn_{0.61}Se$/ZnS.aML (a = 0, 2, 4 and 6), at 300 K, analyzed at emission peak maximum, $\lambda_{exc.}$ = 402 nm.

3.2.2. Photoluminescence of $Cd_{0.38}$ $Zn_{0.62}Se/ZnSe_xS_{1-x}$.4ML quantum dots

The most interesting part of this study is that the results will be presented in the following sections. Figure 7 presents the PL spectra of the CdZnSe/$ZnSe_xS_{1-x}$ 4ML, x = 0.4, 0.5, 0.6 and 0.8) synthesized at 280 °C (20 min). It is alloy core / alloy shell samples series, with the same coating thickness of 4 ML. The FWHM of PL spectra of QDs sample series is quite narrow (~ 26 nm), indicating a good quality of this sample series. The measured PL intensity quantitative comparison is carried out, the samples have the same concentration of QDs. The measurement conditions are kept the same.

With the same thickness of 4 ML, the strongest emission intensity for samples with shell

layer has composition $ZnSe_{0.4}S_{0.6}$, then the fluorescence intensity decreases. Add more of Se into ZnS shell to form the anions alloy shell, change the effective band gap of the crust material and observe the shell composition's impact on the optical properties of the core with same composition. We have observed some interesting phenomenon, which is the significant increase in PL intensity with the shell composition (up to ratio Se/S = 0.4/0.6), then the reduction in emission intensity. Moreover, the emission color and peak was also shifted towards longer wavelengths, from 559 nm to 602 nm, this shows that we can change the emission color from green to orange-red simply by changing shell ingredients. The FWHM is also changed to follow the x value: $Cd_{0.38}Zn_{0.62}Se$ core: the emission peak at 559 nm and FWHM is 25.5 nm, $Cd_{0.38}Zn_{0.62}Se$ /$ZnSe_{0.4}S_{0.6}$: (x = 0.4) the peak at 602.2 nm, FWHM = 43.4 nm, x = 0.5: the peak at 584.4 nm, FWHM = 36.3 nm, x = 0.6: the peak at 575 nm, FWHM = 29.3 nm, x = 0.8: the peak at 575.7 nm, FWHM = 28 nm.

Explanation for the enhancement of fluorescence intensity of alloy QDs come to form a certain composition of shell ZnSeS (example Se/S = 0.4/0.6), as well as change in fluorescent colors, the red shifts with shell composition, which can be attributed to the more number of quantum dots in ON states of this sample. Small spectral changes are also observed in type-I QDs when a finite potential well of the shell allows tunneling of the electron and hole between the core and the shell [33-35].

For the lifetime, unlike the case presented in Fig. 6, the decay curves of $Cd_{0.38}Zn_{0.62}Se/ZnSe_xS_{1-x}$ nanocrystals at room temperature shows an opposite trend (Fig. 8). When a shell with alloy composition changes, the decay curves become steeper than the decay of the core CdZnSe, mean PL lifetime is shorter than in the $CdZnSe/ZnSe_xS_{1-x}$ nanocrystal, compared to the PL lifetime of CdZnSe core. We need more study to explain this.

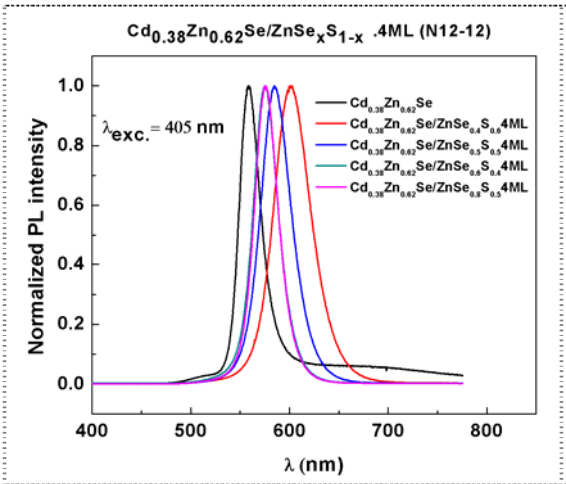

Figure 7. The normalized PL spectra of $CdZnSe/ZnSe_xS_{1-x}$ 4ML, x = 0.4, 0.5, 0.6 and 0.8) synthesized at 240°C. $\lambda_{exc.}$ = 405 nm.

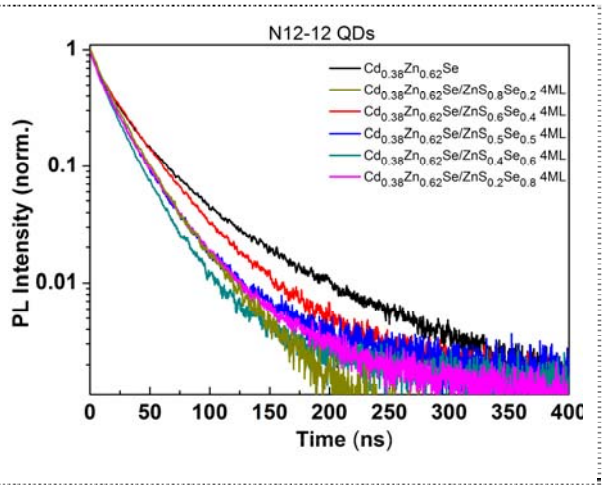

Figure 8. Time-resolved PL decay curves of $Cd_{0.38}Zn_{0.62}Se/ZnSe_xS_{1-x}$.4ML (x = 0, 0.2, 0.4, 0.5, 0.6 and 0.8), at 300K, analyzed at emission peak maximum, $\lambda_{exc.}$ = 402 nm.

3.3. Blinking measurements

To check the quality of the alloy QDs samples, we measured the PL blinking of them. We now use a microscope in order to study the properties of single nanocrystals, and specifically their blinking statistics. A portion of the sample was illuminated at 430 nm by a mercury-vapor

lamp. The sample was imaged by a CCD camera, with a pixel size of 6.3 µm corresponding to a resolution of 63 nm. The CCD rate was of 10 frames per second. We recorded films of 311 frames (30 s duration).

For the sample $Cd_{0.39}Zn_{0.61}Se/ZnS$ 4ML (N8-4-12), we plot in Fig. 9 (left). The intensity as a function of time for 4 QDs: the blinking is quite similar to the CdSe/ZnS nanocrystals. We do the same for 25 nanocrystals. For each nanocrystal, we define manually a threshold above which we consider that the nanocrystal is in the ON state (indicated as a green line in the above figure). For instance, for the four nanocrystals in fig. 10, we choose the thresholds : 5600, 3000, 1800, 5300. We then calculate the fraction of time spent by each nanocrystal in the ON state (above the threshold). We plot a histogram of this fraction (Fig. 9, right). We calculate that, on average, the nanocrystals spend 35 % in the ON time. More specifically, about one third of them are in the ON state more than 50 % of the time, and about one third of them are in the ON state less than 20 % of the time.

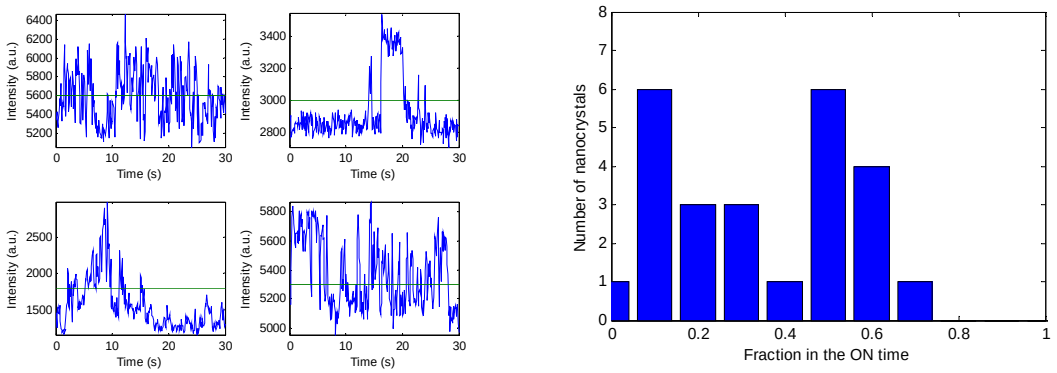

Figure 9. Left: Intensity time traces of four different nanocrystals, measured by CCD camera with a 100 ms resolution for sample $Cd_{0.39}Zn_{0.61}Se/ZnS$ 4ML (N8-4-12) (the threshold between ON and OFF states is plotted in green). In right: Histogram of the fraction of time spent by each nanocrystal in the ON state for the same sample.

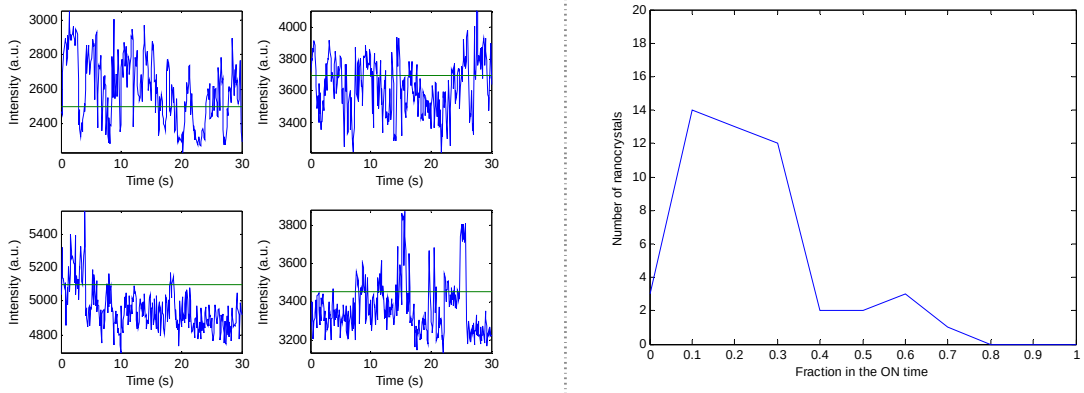

Figure 10 . Left: intensity time traces of four nanocrystals of sample $Cd_{0.38}Zn_{0.62}Se$ (N12-0-12). Right: histogram of the fraction of time spent in the ON state.

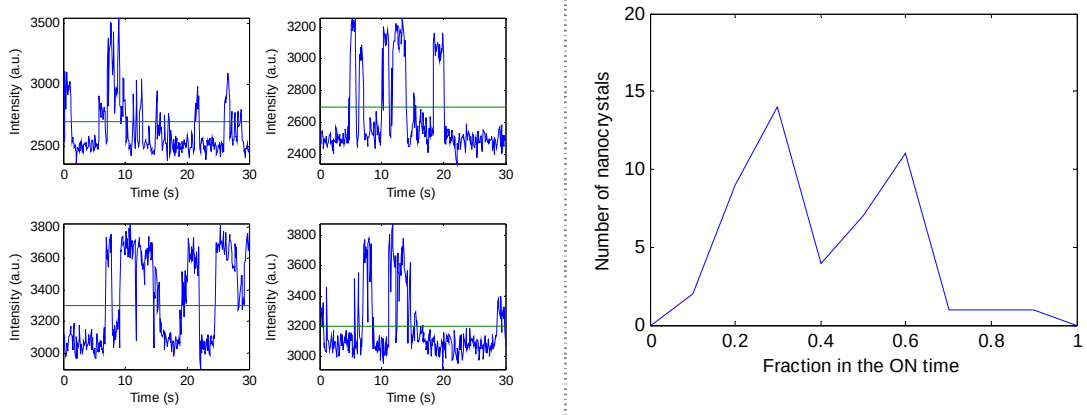

Figure 11. Left: intensity time traces of four nanocrystals of sample $Cd_{0.38}Zn_{0.62}Se$ /$ZnSe_{0.8}S_{0.2}$.4ML (N12-0.8 -4 -12). Right: histogram of the fraction of time spent in the ON state.

To carry out in a similar way, we measured the PL blinking of the other samples. Figures 10 and 11 present the results of PL blinking of the samples $Cd_{0.38}Zn_{0.62}Se$ (N12-0-12) and $Cd_{0.38}Zn_{0.62}Se$ /$ZnSe_{0.8}S_{0.2}$. 4ML.

This was performed by considering 50 nanocrystals for each sample. We thus estimate that the relative statistical error is roughly of the order of sqrt(50)/50 = 1/7 = 15 %. We choose a threshold as explained before and calculate for each nanocrystal its fraction of time spent in the ON state. We report here in the table 1, the results of 4 samples of the series N12 :

- The average of this fraction for all the nanocrystals
- The percentage of nanocrystals for which this fraction is above 50 %
- The percentage of nanocrystals for which this fraction is below 20 %

- *Table 1.* The result involves the calculation ON state of four nanocrystals.

Sample	N12 – 0 – 12 $Cd_{0.38}Zn_{0.62}Se$	N12-0.2-4-12 $Cd_{0.38}Zn_{0.62}Se$ /$ZnSe_{0.2}S_{0.8}$	N12-0.5-4-12 $Cd_{0.38}Zn_{0.62}Se$ /$ZnSe_{0.5}S_{0.5}$	N12-0.8-4-12 $Cd_{0.38}Zn_{0.62}Se$ /$ZnSe_{0.8}S_{0.2}$
Average fraction of ON time (%)	23	36	33	41
% of nanocrystals which are ON more than 50 % of the time	8	22	20	34
% of nanocrystals which are ON less than 20 % of the time	46	16	28	10

We find that N12-0-12 ($Cd_{0.38}Zn_{0.62}Se$) is the least good sample, as expected probably from its structure (no shell) whereas N12-0.8-4-12 ($Cd_{0.38}Zn_{0.62}Se/ZnSe_{0.8}S_{0.2}$) is the best sample (higher average fraction in ON state, more nanocrystals are ON more than half the time, few nanocrystals are OFF more than 80 % of the time).

4. CONCLUSIONS

The first result of the creation of alloy core/shell QDs are presented in this report, allowed to confirm the alloy essence of the crystalline phase in the sample QDs as CdZnSe zinc blend alloy, the presence of the component elements (Cd, Zn, Se) in the QDs and their size (~ 7 nm). We could easily fabricate the QDs emitting green color with high accuracy and reproductible. Quantitative measurements of PL intensity confirmed the coating more thick ZnS shell has increased the intensity with a little changing the spectral peak position. The alloy shell layer with the same thickness, but the composition changes made the emission peak of QDs shifted to red and increasing the emission intensity. The QD PL decay was interpreted in relation with the emitting state fine structure, and a reduction of the non-radiative decay channels by the ZnS shell was also evidenced. By PL microscopy, the blinking of the QDs was studied. It was shown that the QDs spent by the nanocrystal in the ON state ranged typically between 20 and 40 %, and was dependent on the core composition.

Acknowledgments. We sincerely thank Prof. Nguyen Quang Liem for his support. This research is funded by Vietnam National Foundation for Science and Technology Development (NAFOSTED) under grant number 103.06-2011.03, the PICS cooperation project between CNRS and VAST and the support for young researchers from IMS-VAST. The authors thank the National Key Laboratory for Electronic Materials and Devices-IMS for the use of facilities.

REFERENCES

1. Jong-Uk Kim, Jong-Jin Lee, Ho Seong Jang, Duk Young Jeon, and Heesun Yang - Widely Tunable Emissions of Colloidal $Zn_xCd_{1-x}Se$ Alloy Quantum Dots Using a Constant Zn/Cd Precursor Ratio, J. Nanosci. Nanotechnol. **1** (2011) 725-729.
2. Zhengtao Deng, Hao Yan, and Yan Liu – Band Gap Engineering of Quaternary Alloyed ZnCdSSe Quantum Dots via a Facile Phosphine-Free Colloidal Method, J. Am. Chem. Soc. **131** (2009) 17744–17745.
3. Nguyen Hong Quang – Synthesis and optical properties of CdSe nanocrystals and CdSe/ZnS core/shell nanostructures in non-coordinating solvents, Adv. Nat. Sci.: Nanosci. Nanotechnol. **1** (2010) 025004.
4. Ung Thi Dieu Thuy, Pham Song Toan, Tran Thi Kim Chi, Dinh Duy Khang and Nguyen Quang Liem – CdTe quantum dots for an application in the life sciences, Adv. Nat. Sci.: Nanosci. Nanotechnol. **1 (**2010) 045009.
5. Chu Viet Ha, Nghiem Thi Ha Lien, Le Tien Ha, Vu Dinh Lam, Tran Hong Nhung and Vu Thi Kim Lien – Synthesis and optical properties of water soluble CdSe/CdS quantum dots for biological applications, Adv. Nat. Sci.: Nanosci. Nanotechnol. **3** (2012) 025017.
6. Tran Thi Kim Chi, Vu Duc Chinh, Ung Thi Dieu Thuy, Nguyen Hai Yen, Nguyen Ngoc Hai, Dao Tran Cao, Pham Thu Nga and Nguyen Quang Liem – Fabrication of fluorescence-based biosensors from functionalized CdSe and CdTe quantum dots for pesticide detection, Adv. Nat. Sci.: Nanosci. Nanotechnol. **3** (2012) 035008.
7. Nguyen Duc Nghia, Ngo Trinh Tung and Nguyen Quang Liem – Highly sensitive fluorescence resonance energy transfer (FRET)-based nanosensor for rapid detection of clenbuterol, Adv. Nat. Sci.: Nanosci. Nanotechnol. **3** (2012) 035011.
8. Ung Thi Dieu Thuy, Tran Thi Kim Chi, Pham Thu Nga, Nguyen Duc Nghia, Dinh Duy

Khang and Nguyen Quang Liem – CdTe and CdSe quantum dots: synthesis, characterizations and applications in agriculture, Adv. Nat. Sci.: Nanosci. Nanotechnol. **3 (**2012) 043001.

9. Zheng Y. G, Yang Z. C, and Ying J. Y – Quantum Dots: Nanoparticles with Outstanding Fluorescent Properties, Adv. Mater. **19 (2007)** 1475.
10. Zhong X. H, Zhang Z. H, Liu S. H, Han M. Y, and Knoll W – The Supramolecular Chemistry of Organic-Inorganic Hybrid Materials, J. Phys. Chem. **B 108 (2004)** 15552.
11. Zhong X. H, Feng Y. Y, Zhang Y. L, Gu Z. Y, and Zou. L – Alloyed $Zn_xCd_{1-x}S$ Nanocrystals with Highly Narrow Luminescence Spectral Width, Nanotechnol. **18** (2007) 385606.
12. Liu F. C, Cheng T. L, Shen C. C, Tseng W. L, and Chiang M. Y – Synthesis of Cysteine-Capped ZnxCd1-xSe Alloyed Quantum Dots-Emitting in the Blue-Green Spectral Range, Langmuir **24** (2008) 2162.
13. Santangelo S. A, Hinds E. A, Vlaskin V. A, Archer P. I, and Gamelin D. R – Bimodal Bond-Length Distributions in Cobalt-Doped CdSe, ZnSe, and $Cd_{1-x}Zn_xSe$ Quantum Dots , J. Am. Chem. Soc. **129** (2007) 3973.
14. Zhong X. H, Han M. Y, Dong Z. L, White T. J., and Knoll W. – Composition-Tunable $Zn_xCd_{1-x}Se$ Nanocrystals with High Luminescence and Stability, J. Am. Chem. Soc. **125** (2003) 8589.
15. Sung Y. M, Lee Y. J, and Park K. S – Kinetic Analysis for Formation of $Cd_{1-x}Zn_xSe$ Solid-Solution Nanocrystals, J. Am. Chem. Soc. **128** (2006) 9002.
16. Zhong X. H, Feng Y. Y, Knoll W, and Han M. Y – Embryonic nuclei induced alloying process for the reproducible synthesis of blue-emitting $Zn_xCd_{1-x}Se$ nanocrystals with long-time thermal stability in size distribution and emission wavelength, J. Am. Chem. Soc. **125** (2003) 13559.
17. Quyang J. Y., Ratcliffe C. Y., Kingston D., Wilkinson B., Kuijper J., Wu X. H, Ripmeester J. A., and Yu K. – Gradiently Alloyed $Zn_x Cd_{1-x}S$ Colloidal Photoluminescent Quantum Dots Synthesized via a Noninjection One-Pot Approach, J. Phys. Chem C **112** (2008) 4908.
18. Bae W. K., Nam M. K., Char K, and Lee S. – Gram-Scale One-Pot Synthesis of Highly Luminescent Blue Emitting $Cd_{1-x}Zn_xS$/ZnS Nanocrystals, Chem. Mater. **20** (2008) 5307.
19. Bailey R. E. and Nie S. M. – Alloyed Semiconductor Quantum Dots: Tuning the Optical Properties without Changing the Particle Size, J. Am. Chem. Soc. **125** (2003) 7100.
20. Bae W. K., Char K., Hur H., and Lee S. – Single-Step Synthesis of Quantum Dots with Chemical Composition Gradients, Chem. Mater. **20** (2008) 531.
21. Caruge J. M., Halpert J. E., Wood. V., Bulovic V., Bawendi M. G. – Colloidal quantum-dot light-emitting diodes with metal-oxide charge transport layers, Nat. Photonics **2** (2008) 247.
22. Wang X., Ren X., Kahen K., Hahn M. A., Rajeswaran M., Zacher S. M., Silcox J., Cragg G. E., Efros A. L., and Krauss T. D. – *Non-blinking semiconductor nanocrystals*, Nature **459** (2009) 686.
23. Christophe Galland, Yagnaseni Ghosh, Andrea Steinbruck, Milan Sykora, Jennifer A. Hollingsworth, Victor I. Klimov and Han Htoon – Two types of luminescence blinking

revealed by spectroelectrochemistry of single quantum dots, Nature **479** (2011) 203-207.

24. Todd D. Krauss and Jeffrey J. Peterson – Quantum dots: A charge for blinking, Nature Materials **11** (2010) 14-16.
25. Javier Vela, Han Htoon, Yongfen Chen, Young-Shin Park, Yagnaseni Ghosh, Peter M. Goodwin, James H. Werner, Nathan P. Wells, Joanna L. Casson, Jennifer A. Hollingsworth – Effect of shell thickness and composition on blinking suppression and the blinking mechanism in 'giant'CdSe/CdS nanocrystal quantum dots, J. Biophotonics **3** (10–11) (2010) 706–717.
26. Huiguang Zhu, Arjun Prakash, Denise N Benoit, Christopher J. Jones, and Vicki L. Colvin – Low temperature synthesis of ZnS and CdZnS shells on CdSe quantum dots, Nanotechnology **21** (2010) 255604.
27. Hines M. A. and Guyot-Sionnest P. - Synthesis and Characterization of Strongly Luminescing ZnS-Capped CdSe Nanocrystals, J. Phys. Chem. **100** (1996) 468–71.
28. Nga P. T., Chinh V. D., Hanh V. T. H., Nghia N. X., and Dzung P. T. - Optical properties of normal and "giant" multishell CdSe quantum dots for potential application in material science, Int. J. Nanotechnol. **8** (3/4/5) (2011) 347-359.
29. Xie R. G., et al. – Synthesis and Characterization of Highly Luminescent CdSe − Core CdS/$Zn_{0.5}Cd_{0.5}$S/ZnS Multishell Nanocrystals, J. American Chemical Society **127** (20) (2005) 7480-7488.
30. Tran Thi Quynh Hoa, Le Thi Thanh Binh, Le Van Vu, Nguyen Ngoc Long, Vu Thi Hong Hanh, Vu Duc Chinh and Pham Thu Nga – Luminescent ZnS:Mn/thioglycerol and ZnS:Mn/ZnS core/shell nanocrystals: Synthesis and characterization, Optical Materials **35** (2010) 136-140.
31. Li J. J. et al. – Large-Scale Synthesis of Nearly Monodisperse CdSe/CdS Core/Shell Nanocrystals Using Air-Stable Reagents via Successive Ion Layer Adsorption and Reaction, J. Am. Chem. Soc. **125** (2003) 12567–12575.
32. Protiere M. and Reiss P. – Highly luminescent Cd1-xZnxSe/ZnS core/shell nanocrystals emitting in the blue-green spectral range, Small **3** (3) (2007) 399-403.
33. Andrew M. Smith, Aaron M. Mohs and Shuming Nie – Tuning the Optical and Electronic Properties of Colloidal Nanocrystals by Lattice Strain, Nature nanotechnology **4** (2009) 56-64.
34. Dabbousi B. O., et al. – (CdSe)ZnS Core−Shell Quantum Dots: Synthesis and Characterization of a Size Series of Highly Luminescent Nanocrystallites, J. Phys. Chem. B **101** (1997) 9463–9475.
35. Peng X. G., Schlamp M. C., Kadavanich A. V., and Alivisatos A. P. – Epitaxial Growth of Highly Luminescent CdSe/CdS Core/Shell Nanocrystals with Photostability and Electronic Accessibility, J. Am. Chem. Soc. **119** (1997) 7019–7029.

TÓM TẮT

TỔNG HỢP VÀ SO SÁNH QUANG HUỲNH QUANG CỦA CÁC CHẤM LƯỢNG TỬ HỢP KIM CdZnSe/ZnS VÀ CdZnSe/ZnSeS

Nguyễn Hải Yến[1, *], Nguyễn Ngọc Hải[1], Lê Văn Vũ[2], Phan Tiến Dũng[1],

Nguyễn Xuân Nghĩa[1], Laurent Coolen[3, 4], Pham Thu Nga[1]

[1]*Viện Khoa học vật liệu, Viện HLKHCNVN, 18 Hoàng Quốc Việt, Cầu Giấy, Hà Nội*

[2]*Trung tâm Khoa học vật liệu, Khoa Vật lý, Trường Đại học Khoa học tự nhiên, Đại học Quốc gia, 334 Nguyễn Trãi, Thanh Xuân ,Hà Nội*

[3]*Đại học Sorbonne, Đại học Paris 06,UMR 7588, Viện Khoa học Nano Paris, F – 75005, Paris - Pháp*

[4]*Viện Khoa học Nano Paris, F – 75005, Paris - Pháp*

[*] Email*: haiyen@ims.vast.ac.vn*

Để phục vụ việc tìm kiếm các cấu trúc và thành phần mới của các chấm lượng tử, ngăn chặn các hiện tượng nhấp nháy (sự thay đổi ngẫu nhiên giữa các trạng thái phát xạ cao (on) và trạng thái phát xạ thấp (off) dưới sự kích thích liên tục các điện tử) và phục vụ các mục đích ứng dụng trong y-sinh học, các thiết bị quang điện, chúng tôi đã nghiên cứu chế tạo các chấm lượng tử hợp kim (QDs). Trong bài báo này, chúng tôi trình bày các kết quả mới về hợp kim chấm lượng tử có cấu trúc lõi/vỏ với lớp vỏ là hợp kim và có hàm lượng thành phần thay đổi, đó là các chấm lượng tử hợp kim CdZnSe/$ZnSe_xS_{1-x}$ aML với x (x = 0; 0,2; 0,4; 0,5; 0,6; 0,8) và lớp vỏ có chiều dầy aML (a = 2, 4, 6). Phổ huỳnh quang và cường độ phát xạ của chúng thay đổi theo thành phần của lớp vỏ. Độ bán rộng phổ (FWHM) của phổ phát xạ của các chấm lượng tử hợp kim lõi CdZnSe là 25,5 nm. Sau khi được bọc vỏ thì cường độ của lõi hợp kim CdZnSe tăng theo chiều dày của lớp vỏ. Với mục đích so sánh tác dụng của hai loại vỏ khác nhau trên cùng một loại chấm lượng tử hợp kim lõi. Các vật liệu vỏ là ZnS và ZnSeS đã được sử dụng trong bài báo này. Khi phủ bên ngoài hợp kim lõi một lớp hợp kim vỏ ZnSeS thì cùng với một chiều dầy như nhau nhưng các bước sóng và cường độ của các chấm lượng tử hợp kim cũng thay đổi khi thay đổi hàm lượng thành phần của lớp vỏ. Kết quả cũng chỉ ra rằng các chấm lượng tử hợp kim ở trạng thái bật "ON" của tinh thể thường dao động vào khoảng từ 20 đến 40 % và phụ thuộc vào thành phần của chấm lượng tử hợp kim lõi. Các kết quả thực nghiệm cũng được trình bày và thảo luận một cách chi tiết trong bài báo.

Từ khóa: chấm lượng tử hợp kim, tổng hợp, tinh thể nano, cấu trúc lõi/vỏ, phát xạ huỳnh quang, CdZnSe/ZnSeS.